Stabilization of unstable rigid rotation of spiral waves in excitable media

J. Schlesner, V. Zykov, H. Engel, and E. Schöll
Institut für Theoretische Physik, Technische Universität Berlin, Hardenbergstrasse 36, D-10623 Berlin, Germany
(Received 19 April 2006; published 24 October 2006)

Depending on the parameters of two-dimensional excitable or oscillatory media rigidly rotating or meandering spiral waves are observed. The transition from rigid rotation to meandering motion occurs via a supercritical Hopf bifurcation. To stabilize rigid rotation in a parameter range beyond the Hopf bifurcation, we propose and successfully apply a proportional control algorithm as well as time delay autosynchronization. Both control methods are noninvasive. This allows for determination of the parameters of unstable rigid rotation of spiral waves either for a model or an experimental system. Using the Oregonator model for the light-sensitive Belousov-Zhabotinsky reaction as a representative example we show that quite naturally some latency time appears in the control loop, and propose an efficient method to overcome its destabilizing influence.

DOI: 10.1103/PhysRevE.74.046215 PACS number(s): 82.40.Bj, 47.54.−r, 05.65.+b

I. INTRODUCTION

Spiral waves represent typical two-dimensional spatiotemporal patterns in nonlinear media. They have been observed in a large variety of excitable or oscillatory reaction-diffusion systems. Well-known examples include cardiac muscle tissue [1,2], aggregating slime-mold cells [3], catalytic surface reactions as the oxidation of carbon monoxide on a platinum single crystal surface [4], or concentration waves in the Belousov–Zhabotinsky (BZ) reaction [5–12].

Rotating spiral waves induce spatio-temporal oscillations in the whole medium. Different regimes of rotation have been observed for spiral waves which can be characterized by the trajectory described by the spiral tip [9,11]. The simplest case is a periodic regime called *rigid rotation* with a tip moving along a circle. Rigidly rotating spiral waves have constant shape and rotate uniformly. Under certain conditions a transition from one-frequency periodic to two-frequency quasi-periodic motion occurs where the spiral tip meanders rather than follows a circular orbit. Meandering spiral waves appear in two types called *outward* and *inward meandering* depending on whether their tip trajectory forms a flower-like orbit with loops pointing outwards or inwards, respectively. More complicated *hypermeandering* motion has been reported that includes at least three incommensurate frequencies [13]. Also, the existence of chaotic dynamics cannot be excluded [14].

The theory of spiral waves has been intensively developed during the last years [15–26] but is still far from being complete. It was shown that the transition from rigid rotation to meandering motion is a supercritical Hopf bifurcation. Beyond the bifurcation point, rigidly rotating spiral waves are still a solution of the underlying equations which, however, is unstable. As for any complicated nonlinear system a very important step in the analysis of spiral dynamics is to determine the parameters of rigidly rotating spirals considered as steady states in a corotating reference frame. These parameters as, for example, their rotation frequency and their core radius can be computed by use of standard procedures, if the underlying model equations are known [10,16,21,26]. However, up to now there are no methods to identify the parameters of these unstable solutions in experimental systems. To determine these parameters an unstable two-dimensional spatiotemporal pattern has to be stabilized by use of a noninvasive control method.

Stabilization of strongly meandering spiral waves can have also a practical meaning, since such spirals break down, producing new interactive vortices that evolve into spatiotemporal irregularity, e.g., cardiac arrythmias [14].

Recently, proportional feedback control (PFC) has been successfully applied to stabilize wave segments propagating in a two-dimensional excitable medium [27]. In a circular domain, PFC can force a rigidly rotating spiral wave to move towards the domain center [28]. However, in application to meandering spiral waves this type of feedback control has not been studied so far.

On the other hand the instability of rigid rotation can be viewed as a transition from a stable to an unstable periodic orbit (UPO) [16,20–24]. Noninvasive feedback methods like time delay autosynchronization (TDAS) [29,30] are successfully employed to stabilize UPOs in dynamical systems [31–33]. TDAS is especially efficient and well-studied theoretically in the case when all dynamical variables can be observed and controlled simultaneously [34]. Here the term *noninvasive* refers to the fact that the intrinsic UPO is not changed by the control term, and the control force vanishes when the orbit is reached.

In spatially extended media either the system variables can be monitored only at a finite number of points, or spatially or temporally averaged variables are measured. The control signal is usually applied locally at several points or globally. In spite of these restrictions, there are many examples of successful control by TDAS in one-dimensional media [35–39]. In two- or three-dimensional systems, only a few examples for the stabilization of spatiotemporal patterns by TDAS are known [40].

In this paper, we study feedback-mediated stabilization of rigidly rotating spiral waves in a parameter regime where in the absence of feedback rigid rotation is unstable and meandering spiral waves are observed. For stabilization we propose two noninvasive control methods, proportional and time delayed feedback control, and demonstrate their successful operation in application to spiral wave solutions obtained

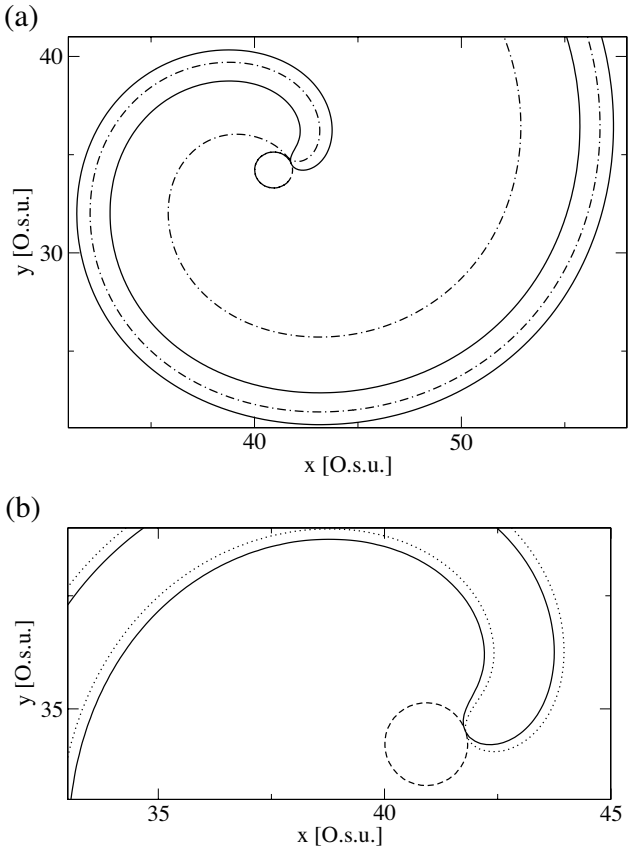

FIG. 1. (a) Isoconcentration lines of the u (solid line) and v field (dash-dotted line) of a rigidly rotating spiral wave. The tip follows the dashed circular trajectory. (b) Tip coordinates are obtained from the intersection between two isoconcentration lines of the u field corresponding to time t (solid line) and time $t+50\Delta t$ (dotted line).

numerically from the Oregonator model for the light-sensitive BZ medium. The latter has been widely used to test feedback-mediated methods for the control of spiral wave dynamics [15,41,42].

Working with real systems, as a rule some control loop latency is unavoidable. Latency effects can deeply influence the operation of the control algorithm [43,44]. For the BZ system we address this issue in some detail and propose a method to compensate possible latency effects to facilitate the experimental verification of our results.

II. THE MODEL

A prominent example for the propagation of spiral waves is the light-sensitive BZ medium. Many experimental studies devoted to the control of spiral wave dynamics have been performed within this system. For our numerical simulations we use the modified two-variable Oregonator model for the BZ reaction given by the equations

$$\frac{\partial u}{\partial t} = \frac{1}{\epsilon}\left(u - u^2 - (fv + \phi)\frac{u-q}{u+q}\right) + D_u \Delta u, \qquad (1)$$

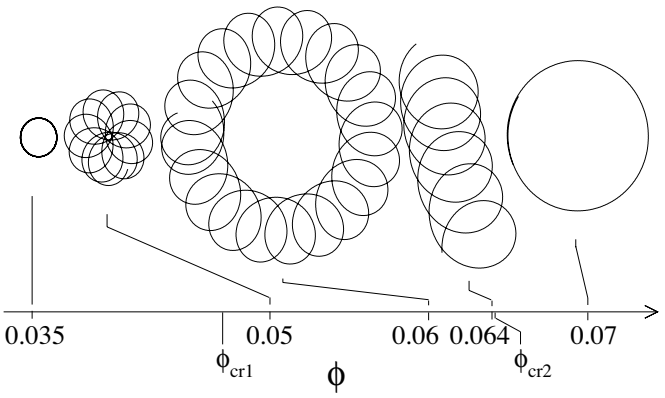

FIG. 2. Tip path patterns obtained under variation of the bifurcation parameter ϕ. In the meandering regime $\phi_{cr1} < \phi < \phi_{cr2}$, rigidly rotating spiral waves are unstable.

$$\frac{\partial v}{\partial t} = u - v + D_v \Delta v. \qquad (2)$$

Here, $u(x,y,t)$ and $v(x,y,t)$ represent the dimensionless concentrations of the activator bromous acid $HBrO_2$ and the oxidized form of the catalyst, respectively, q, f, and $\epsilon \ll 1$ are scaling parameters, and D_u and D_v denote the diffusion constants [45,46]. The photochemically induced bromide flow ϕ is assumed to be proportional to the applied light intensity. Below, ϕ will be considered as the main bifurcation parameter which governs the transition from rigidly rotating to meandering spiral waves.

To obtain spiral wave solutions of the Oregonator model, appropriate initial conditions have to be chosen for the numerical integration of Eqs. (1) and (2) as described in [9], for example. Figure 1(a) shows isoconcentration lines of a rigidly rotating spiral wave computed with parameters $q=0.002$, $f=1.4$, $\epsilon=0.02$, $D_u=1.0$, $D_v=0.6$, and $\phi=0.045$. Except for ϕ, these parameters are kept fixed throughout the paper. Simulations were performed by the forward Euler method using the five-point finite-difference representation of the Laplacian with a spacing $\Delta x=\Delta y=0.125$ O.s.u. (Oregonator space unit) and a time step $\Delta t=0.00125$ O.t.u. (Oregonator time unit).

Solid and dash-dotted lines in Fig. 1(a) represent a snapshot of the isoconcentration lines of the u field at $u_c=0.35$ and of the v field at $v_c=0.11$, respectively. The spiral wave rotates clockwise, and the spiral wave tip moves with constant velocity along the boundary of the circular core shown by the dashed line. As the velocity of the tip in the normal direction to the core boundary is equal to zero, we can define the tip coordinates from the intersection between isoconcentration lines corresponding to two neighboring time instants t and $t+\Delta t$, as illustrated in Fig. 1(b). We use this definition of the spiral tip in our computations below.

Different parameters in the Oregonator model (1), (2) result in rigidly rotating, meandering or hypermeandering spiral wave solutions [10,12]. For fixed values of q, f, ϵ, D_u, and D_v (see above), the regime of rotation is uniquely defined by the parameter ϕ. The bifurcation scenario obtained under variation of ϕ is shown in Fig. 2. At $\phi=0.035$ the

spiral is in the regime of rigid rotation. Increasing ϕ, at $\phi = \phi_{cr1} \approx 0.047$ a supercritical Hopf bifurcation occurs and rigid rotation is replaced by outward meandering. When ϕ grows further, the regime of outward meandering transforms to inward meandering. Finally, after crossing the threshold $\phi_{cr2} \approx 0.0643$ of a second supercritical Hopf bifurcation, rigid rotation is recovered again.

Following [47] we represent the tip path in the meander regime as a superposition of two circular motions with radii r_1, r_2, and frequencies ω_1, ω_2. In this representation the tip coordinates are given by

$$x(t) = r_1 \sin(\omega_1 t + \phi_1) + r_2 \sin(\omega_2 t + \phi_2) + c_1, \quad (3)$$

$$y(t) = r_1 \cos(\omega_1 t + \phi_1) + r_2 \cos(\omega_2 t + \phi_2) + c_2. \quad (4)$$

A detailed analysis performed in [13,47] demonstrates the validity and high accuracy of this representation near the Hopf bifurcation. For rigid rotation we put $r_2 = 0$. The parameters r_1, r_2, ω_1, and ω_2, in contrast to the constant parameters ϕ_1, ϕ_2, c_1, and c_2, change under variation of ϕ. To obtain these dependencies we have fitted our numerical data for the tip trajectories to the above equations.

The full line in Fig. 3(a) shows the sum $r_1 + r_2$ as a function of ϕ. As follows from Eqs. (3) and (4), the sum determines the radius of an envelope surrounding the meandering trajectory. The size of the meandering pattern tends to infinity when ϕ approaches the value $\phi_{ll} \approx 0.0634$. Then, the spiral core drifts along a straight line. This regime marks the transition from outward to inward meandering. The variation of the frequencies ω_1, ω_2 with ϕ is plotted in Fig. 3(b). At the first bifurcation point a second frequency $\omega_2 > 0$ (dashed line) appears, which is quite different from ω_1 (full line). This frequency decreases with increasing ϕ, vanishes at ϕ_{ll}, and becomes negative. The change in the sign reflects the transition from outward to inward meandering. At $\phi = \phi_{cr2}$, this second frequency disappears as the meandering regime ends and rigid rotation becomes stable again.

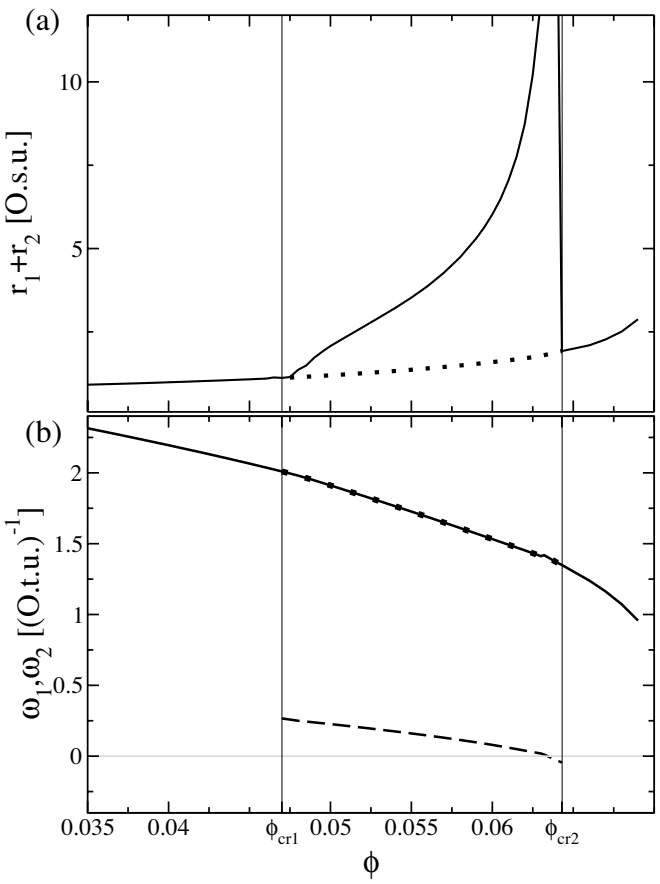

FIG. 3. (a) The sum of the radii of a meandering tip trajectory $r_1 + r_2$ vs the control parameter ϕ. The dotted line denotes the radius r_1 of unstable rigid rotation in the meandering regime. (b) Dependence of the frequencies ω_1 (thick full line) and ω_2 (dashed line) on ϕ. The dots represent the frequency of unstable rigid rotation in the meandering regime between the two Hopf bifurcations.

III. PROPORTIONAL FEEDBACK

Characteristic for rigid rotation is a constant distance r_0 between the tip and the core center of the spiral wave. To suppress the meandering instability, we propose to apply a control force that is proportional to the difference between the actual distance from an arbitrarily chosen reference point, $r(t)$, and the desired radius r_0 according to

$$\phi(t) = \phi_0 + F(t) = \phi_0 + K[r_0 - r(t)]. \quad (5)$$

Here, $F(t)$ denotes the control force and K is the feedback strength. In experiments with the light-sensitive BZ medium, this feedback loop can be realized by changing the intensity of globally applied illumination accordingly; in this case ϕ_0 corresponds to some fixed background illumination. It is important for the control method that the radius r_0 depends on the background illumination ϕ_0. Let us assume first that the relation $r_0 = r_0(\phi_0)$ is known. The more general case of an unknown relationship will be considered later in Sec. V.

Figure 4(a) displays the tip trajectory calculated from Eqs. (1) and (2) in the presence of PFC given by Eq. (5). The cross marks the reference point. Initially, when the feedback strength is zero, the tip follows a path characteristic for outward meandering (dashed line). At $t = 25$ O.t.u. the feedback is switched on. Now, the tip moves along the full line demonstrating that, after a short transient, the tip becomes attracted to a circular orbit of radius r_0 centered at the reference point. Thus rigid rotation is stabilized in a parameter regime where it is unstable in the absence of feedback. In the stabilized regime the control force vanishes, compare to Fig. 4(b). Hence the proposed control method stabilizes an existing unstable periodic orbit (UPO) and does not induce a new periodic solution.

We have performed such stabilization for different values of the control parameter ϕ_0 within the meandering regime $\phi_{cr1} < \phi < \phi_{cr2}$. The dots in Fig. 3 represent the results obtained for the core radius and the rotation frequency in the feedback-stabilized regime. The quantitative analysis of the simulation data shows that in the whole meandering regime the radius of the stabilized trajectory is equal to r_1 and its frequency coincides with ω_1. Our results demonstrate that it is possible to suppress the meandering instability noninvasively by means of global PFC. In the stabilized regime, the whole medium oscillates periodically at the rotation frequency of the spiral wave.

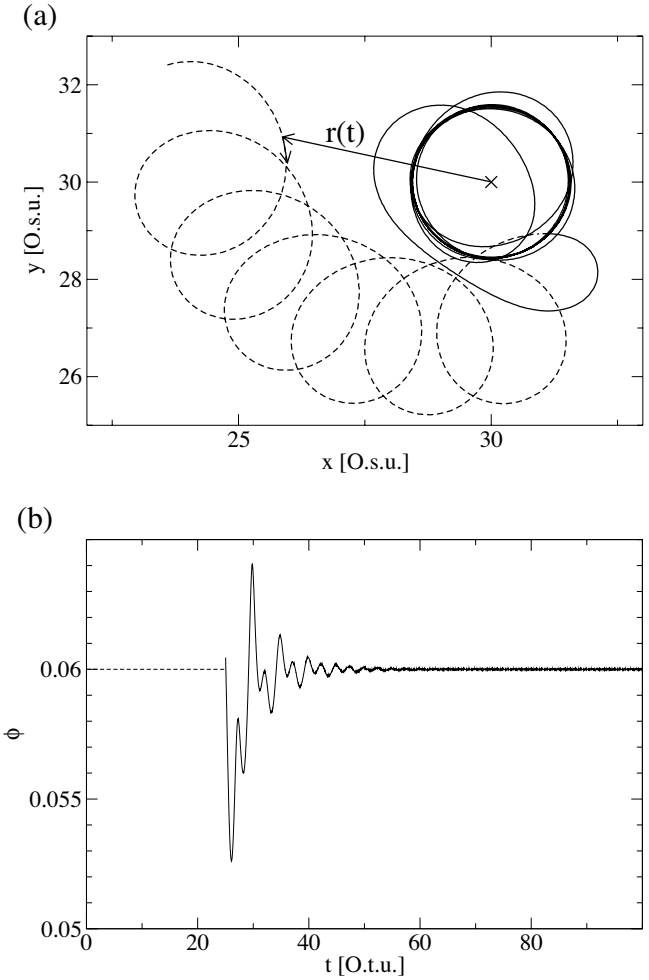

FIG. 4. Stabilization of rigid rotation under proportional feedback control with tip coordinates defined from the u field (u_c =0.35, ϕ_0=0.06). (a) Trajectory of the spiral tip without feedback (K=0, dashed line) and under feedback control (K=0.005, full line) which is switched on at t=25 O.t.u. The cross marks the reference point. (b) Control parameter $\phi(t)$ as a function of time; in the stabilized regime the control force $F(t)$ vanishes.

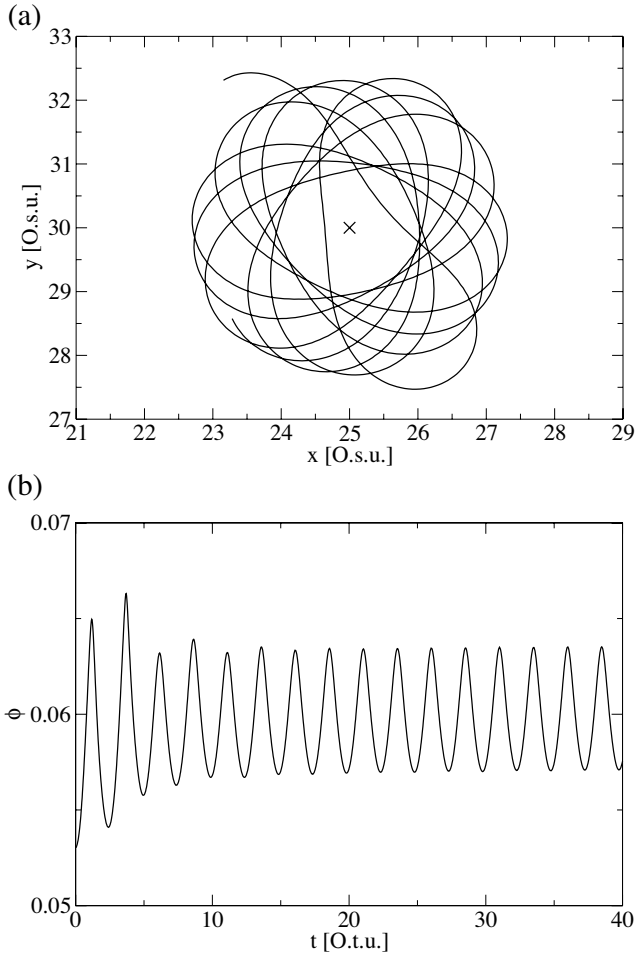

FIG. 5. (a) Tip trajectory under proportional feedback control with tip coordinates defined from the v field. The tip moves to the neighborhood of the reference point (black cross), however, rigid rotation cannot be stabilized. (b) Undamped oscillations of the control force are observed in the asymptotic state.

In light-sensitive BZ media, instead of u the experimentally accessible variable is v. As v is proportional to the oxidized catalytic complex which has a lower absorption coefficient than the reduced complex, in transmitted light areas with high (low) v concentration appear bright (dark). Consequently, in experiments with the BZ medium the coordinates of the spiral tip have to be determined from the measured data for the v field.

We have checked how this modification affects the operation of the feedback algorithm. Figure 5(a) shows the tip trajectory obtained for conditions identical to those used in Fig. 4(a) with the only exception that the tip coordinates are calculated from the isoconcentration lines of the v field. Obviously, under these conditions it is impossible to stabilize rigid rotation in the meandering regime. Asymptotically, the trajectory traced out by the spiral tip is not a circle, although its symmetry center is located at the chosen reference point. Moreover, in the asymptotic state the control force does not vanish but exhibits undamped oscillations. Hence the asymptotic trajectory represents a feedback-induced motion rather than an UPO of the unperturbed system. The same breakdown of the modified feedback algorithm has been observed for other values of the control parameter ϕ_0 within the meandering regime.

To overcome this problem, we propose a simple method that allows one to reconstruct the u field approximately from the v field. Taking into account that v is the slow variable, we neglect the diffusion term in Eq. (2) and define the auxiliary field

$$u_{re}(x,y,t) = \frac{v(x,y,t) - v(x,y,t-\mu)}{\mu} + v(x,y,t). \qquad (6)$$

We set the parameter μ equal to 0.05 O.t.u. which corresponds to a time interval of about 1 s between two consecutive pictures of the v field taken in the experiment. As follows from Fig. 6(a), we succeeded in stabilizing rigid rotation by proportional feedback, provided the tip coordinates were determined from the reconstructed field u_{re}. The

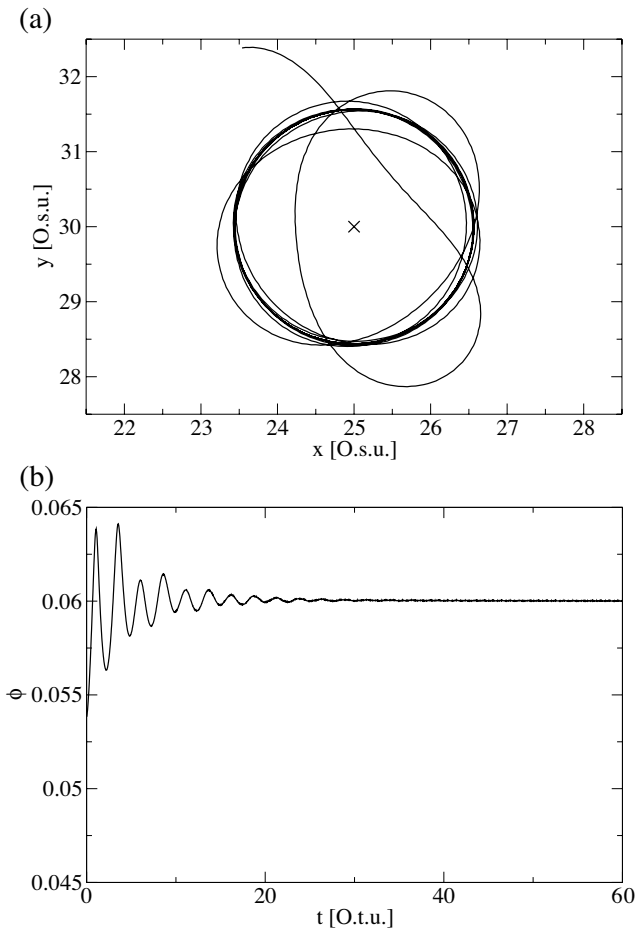

FIG. 6. (a) Successful stabilization of rigid rotation by PFC defining the tip coordinates from the reconstructed activator field u_{re} [Eq. (6) with $\mu=0.05$]. The cross denotes the reference point. (b) Time evolution of the control parameter $\phi(t)$ demonstrating the noninvasive character of the control.

control force vanishes in the stabilized state and ϕ becomes equal to ϕ_0, compare Fig. 6(b).

A closer inspection revealed that latency effects might be responsible for the sensitivity of the control method to different procedures for the definition of the tip coordinates. Note that ϕ enters into Eq. (1) for the activator field of the Oregonator model. Because of time scale separation a perturbation in ϕ affects the inhibitor field with a certain time delay. To give a rough estimate for the delay between u and v in response to a ϕ perturbation we stabilize rigid rotation for a certain ϕ value, say $\phi_0=0.06$. With $u_c=0.35$ and $v_c=0.085$ for the definition of the isoconcentration lines, the radii of the circular tip trajectory calculated from the u and v field are equal. When we switch off the feedback and increase ϕ from 0.06 to 0.061, the tip leaves the circular orbit. Deviations from the circular orbit appear with some time delay and grow initially linearly with time. The trajectory determined from the v field responds with a larger time delay. From the linear growth range we estimate a time delay between u and v equal to $\delta_{uv}\approx 0.13$.

To understand whether a control loop latency δ equal to δ_{uv} is large enough to cause a stabilization failure at ϕ_0

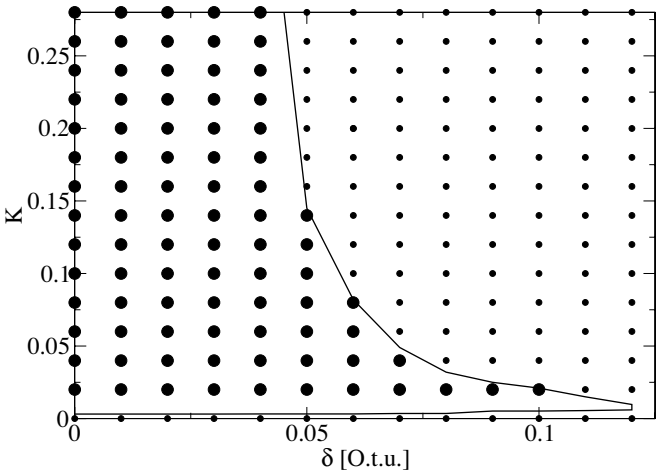

FIG. 7. K-δ diagram for proportional feedback control for $\phi_0=0.06$. Full circles (small dots) denote successful stabilization (failure of stabilization), the boundary of the control domain determined with steps of 0.0005 in the parameter K is marked by the solid line. Tip definition is based on the u field.

$=0.06$, we replace $F(t)$ in Eq. (5) by $F(t-\delta)$. Figure 7 displays the control diagram in the parameter plane spanned by the feedback strength K and the control loop latency δ. As expected the control domain shrinks with increasing latency time. There exists an upper limit $\delta_{cr}=0.12$ for successful stabilization which turns out to be smaller than $\delta_{uv}\approx 0.13$. This proves our conjecture that latency effects cause the breakdown of stabilization as discussed before.

IV. TIME DELAY AUTOSYNCHRONIZATION

PFC is commonly used to stabilize unstable steady states. For the stabilization of UPOs frequently other methods like time delay autosynchronization (TDAS) [29] are employed. Let us check whether this method is applicable to the stabilization of the spiral wave pattern. In the framework of TDAS, the control parameter ϕ is determined as

$$\phi(t) = \phi_0 + F(t) = \phi_0 + K[r(t) - r(t-\tau)]. \qquad (7)$$

To stabilize an unstable periodic orbit with TDAS the time delay τ has to be equal to the period of the UPO which in general is unknown. In our simulations we use the values for the rotation period of rigidly rotating spiral waves stabilized previously under PFC.

One example for successful stabilization by TDAS is shown in Fig. 8. As in Fig. 4, the dashed line denotes the initial part of the simulation performed without control. After the control force has been switched on at $t=25$ O.t.u., the spiral wave is forced into the regime of rigid rotation (full line). In contrast to PFC the center of rigid rotation differs from the chosen reference point, hence asymptotically the distance $r(t)$ is not a constant. Nevertheless, as with PFC, the control force vanishes in the stabilized regime because the actual distance $r(t)$ in Eq. (7) oscillates with period $T\approx\tau$.

To study the robustness of TDAS with respect to latency effects, we account for some latency time δ in the control

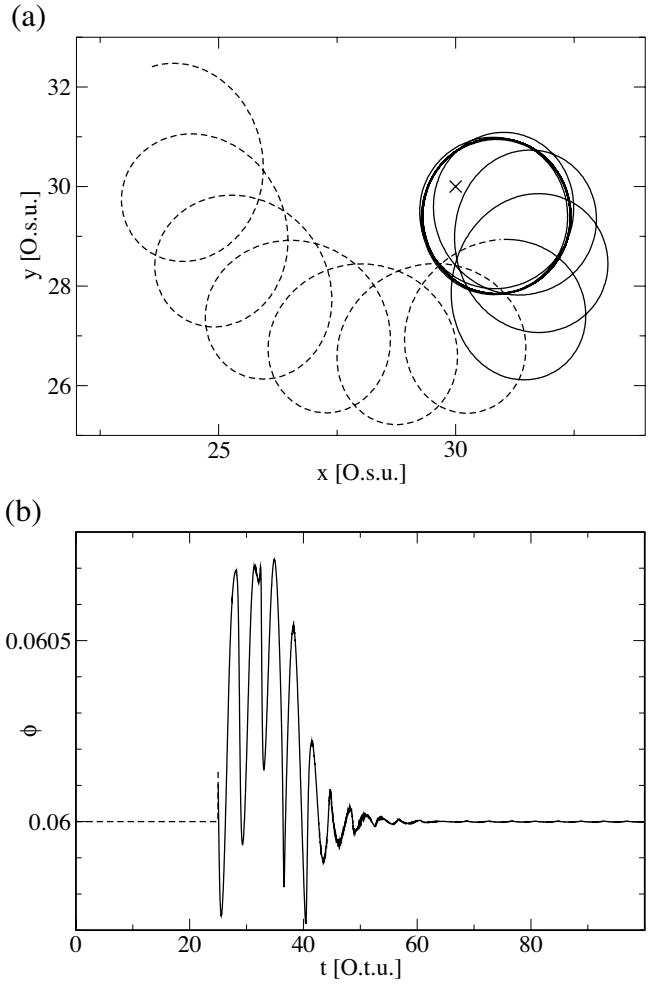

FIG. 8. Stabilization of rigid rotation of a spiral wave applying TDAS with tip location defined from the u field. Parameters: τ =4.015 O.t.u., K=0.001, and ϕ_0=0.06. (a) Trajectory of the spiral tip with and without feedback (dashed and full line, respectively). The cross denotes the reference point. (b) Time evolution of the control parameter $\phi(t)$.

loop replacing $F(t)$ in Eq. (7) by $F(t-\delta)$. In Fig. 9 the boundary of the control domain for the Oregonator model (1), (2) subjected to TDAS is shown by the solid line. As for proportional feedback, the control domain shrinks with δ, but the critical latency δ_{cr} is larger. As $\delta_{cr} > \delta_{uv}$, it should be possible to stabilize rigid rotation with TDAS even when the tip coordinates are defined from the isoconcentration lines of the slower v field. Our simulations have confirmed this conjecture. For suitably chosen control strength, TDAS operates reliably as long as the effective latency $\delta + \delta_{uv}$ is smaller than the critical latency δ_{cr} before it breaks down beyond this limit.

V. COMPARISON OF THE FEEDBACK METHODS

So far we have demonstrated that both PFC and TDAS are capable of stabilizing rigid rotation of spiral waves in the meandering regime. Now, we summarize specific advantages and disadvantages of these two control methods.

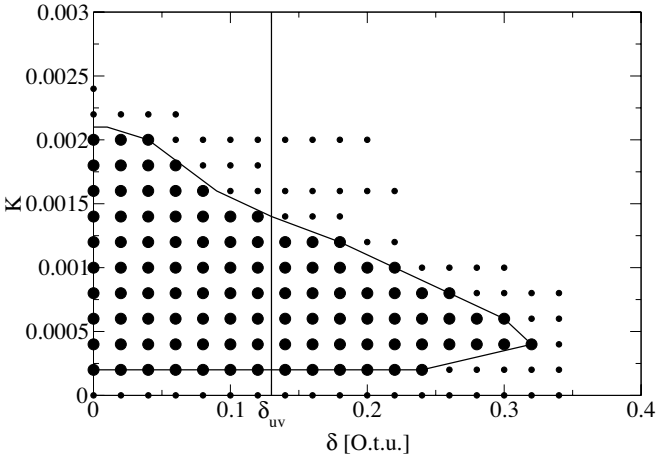

FIG. 9. Control domain for TDAS with tip location defined by the u field for ϕ_0=0.06 and τ=4.015 O.t.u. Full circles denote successful stabilization, small dots denote failure of stabilization.

To apply PFC, in principle the reference radius r_0 must be known. However, we can add simple relaxational dynamics for r_0 according to

$$\frac{dr_0}{dt} = \frac{1}{\epsilon'}[r(t) - r_0] \tag{8}$$

to the model (1), (2) with feedback (5). Provided that r_0 changes on a characteristic time scale much larger than the rotation period of the spiral wave ($\epsilon' \gg T$), this additional equation ensures that r_0 is adapted automatically during feedback-mediated stabilization. In the limit $t \to \infty$, $r_0(t)$ approaches the previously unknown value r_0. In all cases we have checked that the feedback algorithm (5) with the obtained value for r_0 as the initial condition does not change the UPO.

Before we can apply TDAS, we have to identify the period of the UPO to be stabilized, i.e., the rotation period of the spiral wave. Again, τ can be determined solving an additional equation equivalent to Eq. (8) when the control is applied. For the stabilization of rigidly rotating spiral waves, the determination of τ turned out to be numerically more intricate than that of r_0.

For comparison we present in Fig. 10 the control diagrams for PFC and TDAS, which for the given value of the parameter ϕ_0 do not overlap. Feedback strengths required for successful stabilization are smaller with TDAS. In return, the control range in K is larger for PFC. The admitted range of control loop latencies was found to be larger for TDAS which in this respect turns out to be more robust than PFC. Therefore we succeeded in stabilizing rigid rotation with TDAS using information from the slow v field in calculating the tip coordinates, but we failed when we applied PFC due to a control loop latency which was beyond the control boundary.

Note that in PFC the core center of the stabilized rigidly rotating spiral wave always coincides with the arbitrarily chosen reference point. In this respect PFC is capable to move a spiral core to a desired position in the medium.

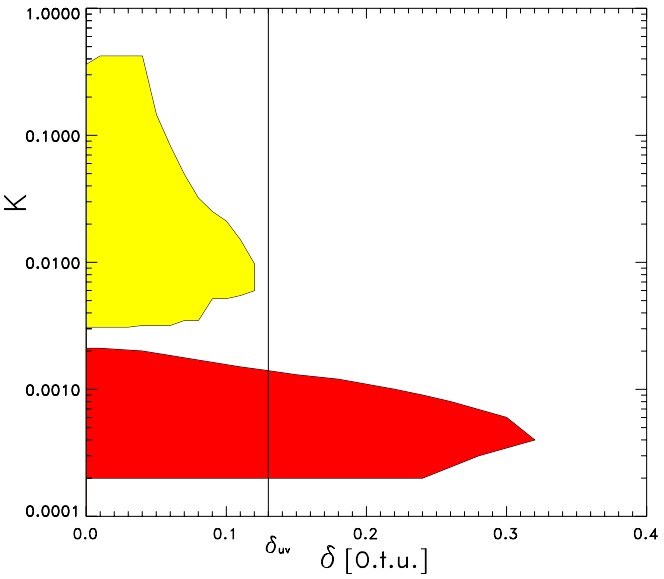

FIG. 10. (Color online) Control domains for proportional feedback (brighter gray, yellow online) and the TDAS (darker gray, red online) for ϕ_0=0.06 and τ=4.015 O.t.u. Half-logarithmic plot.

The control force vanishes in PFC only if $r(t)$ asymptotically approaches a constant value r_0 characteristic for rigid rotation. In contrary, in TDAS periodic oscillations of $r(t)$ are allowed in the stabilized state. Hence it might be possible to stabilize more complicated rotational regimes of spiral waves by TDAS as, for example, meandering spiral waves in the regime of hypermeandering.

VI. SUMMARY AND OUTLOOK

In this paper, we have presented an example for the stabilization of a two-dimensional spatiotemporal pattern by global noninvasive feedback control. A meandering spiral wave is forced into the regime of rigid rotation which still exists but is unstable in the absence of feedback. This allows for determination of the core radius and rotation frequency of unstable rigid rotation without explicit use of the model equations. This opens new perspectives for corresponding experimental studies. Both quantities turn out to be equal to one of the two radii or frequencies, respectively, of spiral meandering which occurs when rigid rotation becomes unstable via a supercritical Hopf bifurcation. It is important to note that from the stabilized two-dimensional spatiotemporal pattern, besides the core radius and the rotation frequency, other characteristics can be obtained as, for example, the spatial profile of the unstable wave or the spatial gradient close to the spiral core. This information could be very helpful in testing the validity of various theoretical approaches to spiral wave dynamics [17,18,25].

The commonly accepted opinion is that the method of tip definition has no pronounced effect on results about spiral wave dynamics as, for example, the bifurcation diagram of the rotation regimes [12]. In the context of feedback-mediated stabilization the situation turns out to be quite different. Sometimes stabilization fails when the tip definition is based on the slow inhibitor instead of the fast activator field. We show that one possible reason for this is the influence of a control loop latency in the feedback loop. To overcome this difficulty we propose an approximate method to reconstruct the activator field from the inhibitor field. This method works well for the Oregonator model of the light-sensitive BZ reaction where only the slow field is experimentally accessible.

Two different noninvasive control methods, proportional feedback control (PFC) and time delayed autosynchronization (TDAS), have been considered in this paper. While both methods allow one to stabilize the wave pattern in a broad range of parameters, a more detailed comparison reveals specific advantages and disadvantages of each method as discussed in Sec. V. PFC requires the determination of some reference radius r_0 which is not as difficult as finding the appropriate delay time τ necessary for TDAS. Moreover, PFC works in a comparably larger range of the feedback strength K, and stabilizes the core center at the reference point. In comparison with that, TDAS is less sensitive to latency effects as the control domain extends to larger latency times, and leads to successful stabilization already at smaller control forces. In principle, TDAS should be able to stabilize two-periodic rotation regimes as meandering spiral waves in the parameter range of hypermeandering [12].

The experimental verification of the predicted stabilization of rigid rotation by noninvasive feedback control remains a challenge for future work. We hope that our results also motivate further development of the general theory of feedback-mediated stabilization of other two-dimensional spatiotemporal patterns.

ACKNOWLEDGMENT

This work was partially supported by DFG in the framework of Sfb 555.

[1] M. A. Allessie, F. I. M. Bonke, and F. J. G. Schopman, Crit. Res. **33**, 54 (1973).
[2] J. M. Davidenko, A. M. Pertsov, R. Salomonsz, W. Baxter, and J. Jalife, Nature (London) **355**, 349 (1992).
[3] G. Gerisch, Naturwiss. **58**, 430 (1971).
[4] S. Jakubith, H. H. Rotermund, W. Engel, A. von Oertzen, and G. Ertl, Phys. Rev. Lett. **65**, 3013 (1990).
[5] A. N. Zaikin and A. M. Zhabotinsky, Nature (London) **225**, 535 (1970).
[6] A. T. Winfree, Science **175**, 634 (1972).
[7] R. J. Field, E. Koros, and R. M. Noyes, J. Am. Chem. Soc. **94**, 8649 (1972).
[8] R. J. Field and M. Burger, *Oscillations and Traveling Waves in Chemical Systems* (Wiley, New York, 1985).
[9] W. Jahnke, W. E. Skaggs, and A. T. Winfree, J. Phys. Chem. **93**, 740 (1989).

[10] *Chemical Waves and Patterns*, edited by R. Kapral and K. Showalter (Kluwer, Dordrecht, 1995).
[11] G. Li, Q. Ouyang, V. Petrov, and H. L. Swinney, Phys. Rev. Lett. **77**, 2105 (1996).
[12] W. Jahnke and A. T. Winfree, Int. J. Bifurcation Chaos Appl. Sci. Eng. **1**, 455 (1991).
[13] T. Plesser and K.-H. Müller, Int. J. Bifurcation Chaos Appl. Sci. Eng. **5**, 1071 (1995).
[14] H. Zhang and A. V. Holden, Chaos, Solitons Fractals **5**, 635 (1995).
[15] A. S. Mikhailov, V. A. Davydov, and V. S. Zykov, Physica D **70**, 1 (1994).
[16] D. Barkley, Phys. Rev. Lett. **68**, 2090 (1992).
[17] V. Hakim and A. Karma, Phys. Rev. E **60**, 5073 (1999).
[18] D. A. Kessler, H. Levine, and W. N. Reynolds, Physica D **70**, 115 (1994).
[19] I. S. Aranson, L. Aranson, L. Kramer, and A. Weber, Phys. Rev. A **46**, R2992 (1992).
[20] D. Barkley, M. Kness, and L. S. Tuckerman, Phys. Rev. A **42**, 2489 (1990).
[21] D. Barkley, Phys. Rev. Lett. **72**, 164 (1994).
[22] B. Fiedler, B. Sandstede, A. Scheel, and C. Wulff, Doc. Math. J. DMV **1**, 479 (1996).
[23] M. Golubitsky, V. G. LeBlanc, and I. Melbourne, J. Nonlinear Sci. **7**, 557 (1997).
[24] B. Sandstede, A. Scheel, and C. Wulff, J. Differ. Eqns. **141**, 122 (1997).
[25] D. Margerit and D. Barkley, Chaos **12**, 636 (2002).
[26] P. Wheeler and D. Barkley, SIAM J. Appl. Dyn. Syst. **5**, 157 (2006).
[27] E. Mihaliuk, T. Sakurai, F. Chirila, and K. Showalter, Phys. Rev. E **65**, 065602(R) (2002).
[28] V. S. Zykov, A. S. Mikhailov, and S. C. Müller, Phys. Rev. Lett. **78**, 3398 (1997).
[29] K. Pyragas, Phys. Lett. A **170**, 421 (1992).
[30] J. E. S. Socolar, D. W. Sukow, and D. J. Gauthier, Phys. Rev. E **50**, 3245 (1994).
[31] W. Just, D. Reckwerth, J. Möckel, E. Reibold, and H. Benner, Phys. Rev. Lett. **81**, 562 (1998).
[32] D. J. Gauthier, D. W. Sukow, H. M. Concannon, and J. E. S. Socolar, Phys. Rev. E **50**, 2343 (1994).
[33] A. Kittel, J. Parisi, and K. Pyragas, Phys. Lett. A **198**, 433 (1995).
[34] W. Just, T. Bernard, M. Ostheimer, E. Reibold, and H. Benner, Phys. Rev. Lett. **78**, 203 (1997).
[35] M. E. Bleich and J. E. S. Socolar, Phys. Rev. E **54**, R17 (1996).
[36] G. Franceschini, S. Bose, and E. Schöll, Phys. Rev. E **60**, 5426 (1999).
[37] N. Baba, A. Amann, E. Schöll, and W. Just, Phys. Rev. Lett. **89**, 074101 (2002).
[38] O. Beck, A. Amann, E. Schöll, J. E. S. Socolar, and W. Just, Phys. Rev. E **66**, 016213 (2002).
[39] J. Schlesner, A. Amann, N. B. Janson, W. Just, and E. Schöll, Phys. Rev. E **68**, 066208 (2003).
[40] O. Lüthje, S. Wolff, and G. Pfister, Phys. Rev. Lett. **86**, 1745 (2001).
[41] V. S. Zykov, G. Bordiougov, H. Brandtstädter, I. Gerdes, and H. Engel, Phys. Rev. E **68**, 016214 (2003).
[42] V. S. Zykov, G. Bordiougov, H. Brandtstädter, I. Gerdes, and H. Engel, Phys. Rev. Lett. **92**, 018304 (2004).
[43] W. Just, D. Reckwerth, E. Reibold, and H. Benner, Phys. Rev. E **59**, 2826 (1999).
[44] P. Hövel and J. E. S. Socolar, Phys. Rev. E **68**, 036206 (2003).
[45] H. J. Krug, L. Pohlmann, and L. Kuhnert, J. Phys. Chem. **94**, 4862 (1990).
[46] J. P. Keener and J. J. Tyson, Physica D **21**, 307 (1986).
[47] G. S. Skinner and H. L. Swinney, Physica D **48**, 1 (1991).